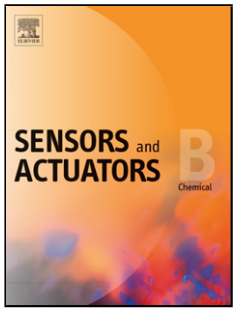

Title: Understanding the Gas Adsorption Kinetics of Langmuir-Schaefer Porphyrin Films Using Two Comparative Sensing Systems

Authors: M. Evyapan, A.K. Hassan, A.D.F. Dunbar

PII: S0925-4005(17)31311-4
DOI: http://dx.doi.org/doi:10.1016/j.snb.2017.07.103
Reference: SNB 22762

To appear in: *Sensors and Actuators B*

Received date: 14-12-2016
Revised date: 12-7-2017
Accepted date: 14-7-2017

Please cite this article as: M.Evyapan, A.K.Hassan, A.D.F.Dunbar, Understanding the Gas Adsorption Kinetics of Langmuir-Schaefer Porphyrin Films Using Two Comparative Sensing Systems, Sensors and Actuators B: Chemicalhttp://dx.doi.org/10.1016/j.snb.2017.07.103

Understanding the Gas Adsorption Kinetics of Langmuir-Schaefer Porphyrin Films Using Two Comparative Sensing Systems

M. Evyapan[1 & 3,*], A.K. Hassan[2] and A. D. F. Dunbar[3]

[1]Department of Physics, University of Balikesir, Balikesir 10145, TURKEY
[2]Materials and Engineering Research Institute, Sheffield Hallam University, Sheffield S1 2NU, UK
[3]Chemical and Biological Engineering, University of Sheffield, Mappin Building S1 3JD UK

Corresponding author: Tel.: +90 266 6121000; fax: +90 2666121215.
Postal address: University of Balikesir, Faculty of Art & Science Department of Physics 10145, Cagis, Balikesir TURKEY
E-mail address: mevyapan@gmail.com (M. Evyapan).

Research Highlights:

- Free base porphyrin based Langmuir-Schaefer (LS) films were fabricated and used as the sensing material for optical VOC sensors.
- A systematic sensor study was performed using two different techniques, namely UV-vis absorbance spectroscopy and surface plasmon resonance (SPR).
- Irrespective of the method used to transduce the response the magnitude of the responses were remarkably similar.
- The sensitivity of the sensor material is largely independent of the measurement system.

Abstract

This study investigated Langmuir-Schaefer (LS) films of a free base porphyrin 5,10,15,20-tetrakis[3,4-bis(2-ethylhexyloxy)phenyl]-21H,23H-porphine (EHO) as sensors to detect acetic acid and methylamine. Such films are known to adsorb VOCs, resulting in a color change and a swelling of the film resulting in a thickness increase for the film. The adsorption kinetics of this process were studied using two different techniques, namely UV-vis absorbance spectroscopy and surface plasmon resonance (SPR), to investigate the color change and film thickness change respectively when exposed to acetic acid and methylamine vapors. These two techniques were used to allow a comparative study to be made of the color change and film swelling in order to enhance understanding of the interaction between the thin films and both acidic and basic vapor molecules.

The transfer process of the LS thin films was performed using the constant transfer pressure of 5 mNm^{-1}. EHO films with different numbers of layers were fabricated and exposed to 855 ppm acetic acid and 900 ppm methylamine vapor. Sensor responses were recorded using both UV-vis and surface plasmon resonance techniques. The EHO films exhibited high sensitivity and fast responses using both techniques. Using two different detection systems permitted the investigation of the interaction mechanism with a quantitative, comparative study with the aim of obtaining an enhanced understanding of the nature of the interaction of the organic vapors with the sensor. The interaction between EHO and the analytes can be considered in terms of three processes which are surface adsorption, diffusion and desorption process. Although both the optical techniques have distinct sensing principles, similar vapor interaction characteristics can be distinguished in both sets of experiments. For both techniques the response to the acid was stronger than the response to methylamine. However, apart from this difference in the magnitude of the responses the interaction with the acid and base were remarkably similar. The sensitivity of the sensor is largely independent of the measurement system.

Keywords: Organic vapor sensor, porphyrin, UV-vis, SPR, vapor adsorption

1. Introduction

Gas sensors will play an increasingly important role in life as awareness of the dangers of indoor and outdoor air pollution increases. Therefore research in the field of gas sensing has become an important issue during the last few decades [1,2]. One group of common air pollutants are toxic VOCs (volatile organic compounds) which are extensively used in daily essentials such as paints, cleaning solvents, plastics, cosmetics and wood preservatives. The vapors of VOCs can be highly dangerous when released after using such products and need to be detected before they reach critical levels in the environment. Therefore there is an increasing demand to develop new sensor devices with increased selectivity and sensitivity compared to existing sensors, ideally at lower cost. Organic materials are widely used as sensing materials with a wide range of specific subsections including polymers [3], calixarenes [4], porphyrins [5] and phthalocyanines [6]. The most important part of any adsorption sensor device is the sensing material which directly interacts with the analyte vapor. Accordingly, most of the research reported on gas sensors is related to development of highly sensitive new sensor materials. However an ideal sensor material should simultaneously demonstrate both high sensitivity and selectivity between analyte vapors. Therefore understanding in detail the interaction between the sensor material and analyte vapor is required to maximize the advantages of using this type of sensor and therefore improve any new sensor devices.

Porphyrin molecules show a distinctive color change upon exposure to VOCs which can be easily detected using ultra-violet to visible (UV-vis) spectroscopy. Moreover, adsorption of vapor molecules by thin film matrix causes swelling of the thin film and the surface plasmon resonance (SPR) technique is capable of detecting these very small thickness changes. These two techniques were studied and the results analyzed in order to obtain a deeper understanding of the sensing process. It is assumed that the vapor molecules first interact with the surface of the sensor film and then diffuse into thin film layers as reported in the literature [7]. These two steps affect the sensor response depending on their intensity and speed.

The main purpose of this study was to investigate the response mechanism when exposed to acetic acid and methylamine in order to develop a deeper understanding of the response mechanism. This was achieved by investigating the intensity, duration and speed of the sensor response using two the different sensing techniques. These analytes were chosen because they both elicit a response from the porphyrin, the molecules are similar in size but differ in the functional groups present (-COOH and -NH_2). Thus the sensor responses can be compared for

both techniques. The two sensor measurement techniques have been widely used in literature but previously always in separate studies. This study is unique in applying these two techniques using the same thin film structures with the same organic vapors in order to directly compare the two techniques.

In this work, a free base porphyrin, 5,10,15,20-tetrakis[3,4-bis(2-ethylhexyloxy)phenyl]-21H,23H-porphine (EHO) was selected as the sensor material because this porphyrin has proven sensitivity to many analytes including alcohols [8], NH_3 [9], acids [10,11], amines [12]. Initially the Langmuir-Schaefer (LS) thin film preparation technique was used to produce EHO films on solid substrates with differing numbers of solid state porphyrin layers. The reproducibility of this process was measured and confirmed by SPR. The sensing properties of these films upon exposure to acetic acid and methylamine were investigated using both UV-vis absorbance spectroscopy and SPR methods. Both methods are highly sensitive and have individually shown remarkable results in previous sensor studies and provide high resolution sensor response results [13,14].

2. Experimental Details

2.1 Materials and LS Film Fabrication

The synthesis and chemical structure of EHO has been described elsewhere [15]. The EHO was dissolved in chloroform at a concentration ~0.5 mg ml^{-1} and the Langmuir-Schaefer (LS) technique was used to transfer different numbers of layers of EHO molecules onto a solid substrate in a precise manner. The chloroform solution of EHO was spread onto an ultrapure water subphase (ElgaPURELab Option >15 MΩcm) using a Hamilton microliter syringe in a NIMA Model 601 BAM Langmuir trough. In order to permit the solvent to evaporate a time period of 15 min was allowed before the area was reduced by closing the trough barriers. Surface pressure - area (Π-A) isotherm graphs were recorded using at a barrier compression speed of 200 cm^2 min^{-1}. All experiments were performed in a cleanroom and at a temperature of ~18 ^oC.

LS films were transferred onto glass slides for the optical UV-vis measurements and 40 nm gold coated glass substrates for the surface plasmon resonance (SPR) measurements. The gold layers were deposited by thermal evaporation onto pre-cleaned glass slides with a deposition rate of 0.2 nm s^{-1} under a vacuum of 10^{-6} Torr. All substrates were subsequently exposed to 1,1,1,3,3,3-hexamethyldisilazane (HMDS) vapor for min 12 h in order to render the surface of

the substrate hydrophobic prior to deposition. Before the deposition process, the monolayer on water surface was compressed to the selected constant surface pressure of 5 mNm^{-1}. The monolayer floating on the water surface was transferred onto the solid substrates by contacting the substrate horizontally onto the floating monolayer and subsequently lifting off a single LS layer. The substrate speed used was 10 mm min^{-1} during the transfer. Each LS layer was allowed to dry for 5 min between subsequent depositions and the surface pressure was allowed to return to the target pressure between each deposition by controlling the trough barrier position. This process was repeated the required number of times in order to produce a multilayer LS film.

2.2 Optical Measurement Systems

In order to investigate the vapor adsorption kinetics of EHO LS films two different optical gas sensing measurements were used to carry out a comparative study. The first one is UV-vis absorbance spectroscopy which was performed using a Mikropack MiniD2 UV–vis–IR light source and an Ocean Optics USB2000 spectrometer. Absorbance spectra of EHO LS films were recorded in the range of 350-800 nm. The second measurement was made using a SPR system which consists of a Kretschmann configuration custom built optical setup [16] incorporating a semi-cylindrical prism (refractive index of 1.515) and optical laser (wavelength of 632.8 nm) the details of which have already been described in another study [17]. A gas cell (PTFE - polytetrafluoroethylene) sealed with a rubber O-ring were integrated to the SPR setup which was placed on the LS films and the reflected light intensity was measured as a function of angle or time depending on the measurement type. The thicknesses of the LS films were evaluated by fitting the SPR curves based on the Fresnell equations. The fitting procedure was achieved using the Winspall 3.01 software which was produced by the Max-Planck Institute [18].

2.3 Vapor sensing measurements

The investigation of the kinetic adsorption of EHO LS films involved recording the dynamic response upon exposure to the analyte vapor. Acetic acid and methylamine vapors were chosen as analytes because they permit a comparison of the sensing response measured using two similar sized molecules with different functional groups. Both analytes have $-CH_3$ functional groups but differ in the one has a -COOH group and the other an $-NH_2$ group. This

allows the study to investigate the influence of functional group on the sensor responses and the nature of the adsorption. The analytes were obtained from Sigma-Aldrich and dry nitrogen was used as the carrier and diluent gas in the UV-vis absorbance spectroscopy measurements.

The UV-vis gas sensing measurement setup contains a purpose built gas exposure chamber connected to two Tylan FC-260 mass flow controllers [19]. The analyte in its liquid phase was contained in a small vessel and a mass flow controller was used to deliver a controlled amount of clean dry nitrogen to the vessel. The analyte vessel was maintained at a known temperature in a temperature controlled water bath. When the nitrogen gas passes through the headspace in the vessel it mixes with the analyte vapor present in the headspace and delivers the analyte vapor to the exposure chamber. The concentration of the analyte vapor was subsequently determined in ppm using the known Antoine parameters to determine the partial pressure at the known temperature [20]. The sample was positioned on a Peltier device and the recovery cycle was carried out by gently heating the sample during the exposure to dry nitrogen. During the recovery cycle, the heating process was sustained for only the first 5 min before the sample temperature was reduced such that is had cooled down to its initial temperature prior to subsequent exposures. The exposure cycles were performed at ~20 ^{o}C and the sensor recovery was conducted at ~50 ^{o}C. The temperatures were measured by a thermocouple attached to the top surface of the Peltier device. The kinetic response as observed by UV-vis absorbance of the samples upon exposure to the analyte vapor was recorded by measuring the change in the absorbance spectrum as a function of time. The measurements of kinetic response were started with a recovery cycle for 10 min and then the analyte vapor was directed into the exposure chamber for 20 min periods. Recovery cycles were limited to only 10 min although the exposure cycles were 20 min in order to observe the saturation points.

In order to perform the SPR sensing measurements SPR curves of LS films were recorded before and after vapor exposure. The exposure to analyte vapor was carried out by injecting a known volume of the analyte vapor into the gas cell using a microsyringe. The required concentration of analyte vapor was prepared before injection. Precise amounts of liquid analyte were transferred into a 2 L glass bottle and then evaporated by gently heating. The concentration of the analyte vapors were calculated using the gas law [21]:

$$c = \frac{22.4\rho T V_s}{273 M V} \times 10^3 \qquad (1)$$

where c is the concentration (ppm), ρ is the density of the liquid sample (g mL^{-1}), T is the temperature of container (K), V_s is the volume of the analyte solution (μL), M is the molecular weight of analyte (g) and V is the container volume (2 L). In order to compare the adsorption kinetics of analyte vapors, concentrations were fixed at constant values which were 855 ppm for acetic acid (CH_3COOH) and 900 ppm for methylamine (CH_3NH_2) for all sensing experiments. Dry air was used as the diluent gas for SPR measurements. An interaction time of 20 min was allowed after injection of vapor into the gas chamber before the post exposure SPR curve was recorded. A constant angle (Θ=49º) was obtained from the linear region of the SPR curve and close to the resonance angle. The kinetic measurements were performed by fixing the incident angle at that constant value and recording the reflected light intensity as a function of time.

3. Results and Discussion

3.1 Film Preparation and Characterization

The monolayer behavior of EHO on a water surface has been investigated previously and reported in the literature [22]. It has been reported that on the water surface EHO molecules tend to aggregate and organize themselves facing each other edge on to the surface, which results in a small area per molecule [23,24]. A shoulder in the surface pressure versus area isotherm associated with this transition has been reported to start at surface pressures over 6 mNm^{-1} [19]. Therefore the transfer process of the LS thin films was performed using a lower constant transfer pressure of 5 mNm^{-1} in an attempt to maximize the proportion of EHO molecules that lying flat and therefore available to interact with the analyte vapors upon transfer to a solid substrate.

Several multilayer EHO LS films were fabricated on gold coated substrates and Fig.1 shows the SPR curves of these films. The SPR curves give the variation of reflected light intensity versus angle of incidence and the minimum reflected light intensity value corresponds to the SPR angle (θ_{SPR}). Coating a gold surface with an organic layer causes a shift of the θ_{SPR} to higher angles when compared with bare gold. It is clearly shown that there are observable shifts of the SPR angle after deposition of multilayer EHO films and the magnitude of the corresponding shifts are directly related to the thickness and optical constants of the organic film on the gold surface. The relation can be given by the following expression [25]:

$$\Delta\theta = \frac{(2\pi/\lambda)(|\varepsilon_m|\varepsilon_i)^{3/2} d}{(n_p \cos\theta)(|\varepsilon_m| - \varepsilon_i)^2 \varepsilon}(\varepsilon - \varepsilon_i) \quad (2)$$

where λ is the wavelength of the laser beam (λ=632.8 nm), n_p is the refractive index of the semi-cylindrical prism, $|\varepsilon_m|$ is the modulus of the complex dielectric constant of the gold film, ε_i is the dielectric constant of the medium in contact with thin film, ε is the film's dielectric constant, and d is organic film thickness.

The values of the SPR shifts ($\Delta\theta$) and the thicknesses were determined by fitting the SPR curves using Winspall 3.02 software and the results are summarized in the inset of Fig.1 for all layer numbers. It is clear that the average monolayer thickness increases with increasing number of layers. Taking the gradient of the straight line fitted to the thickness data in order to estimate the average thickness of each EHO monolayer gives 41 Å. The steadily increasing thickness observed implies that multilayer EHO LS films have been achieved since the film thickness increases monotonically with number of depositions. However this is not the whole story because it appears there are some fluctuations in the thickness of each layer. The number of layers increases the thickness causing an SPR shift but it also results in a broadening of the SPR curve. This type of SPR curve change has previously been seen in literature for multilayer thin films and has been attributed to damping of the resonance due to increasing non-uniformity in the film thickness with increasing number of layers [26,27]. We attribute the non-uniformity in these samples to variations in the orientation of the molecules relative to the substrate. This could be as a result of aggregation and stacking of the porphyrin molecules. Therefore a simple gradient analysis to determine the layer thickness is misleading. Note that the thickness of the 4 layer film is only 66 Å giving an average value of only 16.5 Å for the first 4 layers of EHO film. Much closer to the value of 20 Å which was previously reported for a 6 layer EHO film [19]. Some of the EHO molecules may be deposited side on rather than flat resulting in much thicker regions whilst others lie flat resulting in thinner regions. The results obtained will therefore be an average thickness. This spatial variation in thicknesses results in non-uniform layers which correspond with the broadening of the SPR curves for the thicker and therefore increasingly non-uniform films.

3.2 Sensing Properties

In order to investigate the adsorption kinetics of EHO films the two different optical measurement systems were used and the sensor responses were recorded upon exposure to acetic acid and methylamine vapors. These two distinct chemicals have been chosen to help clarify the adsorption kinetics of EHO films. UV-vis and SPR measurement systems are both very capable of detecting small sensor responses [18,19]. Both are optical techniques but differ in what they measure; while UV-vis detects spectral absorbance changes SPR is sensitive to thickness changes of the organic film. Thus the adsorption kinetics of EHO film can be clarified using the complimentary information available from these optical techniques.

3.2.1 UV-Vis Characterization

UV-vis absorption spectra of EHO have been studied and described previously in the literature [28]. EHO in solution exhibits a distinctive Soret band at 426 nm which upon transfer to a solid substrate broadens and redshifts to about 440 nm. There are also four weaker Q bands between 500 and 650 nm. This shift has been attributed to changes in the local environment of the EHO molecules, which may be due to aggregation and/or removal of the solvent. When EHO is exposed to an equal concentration of each analyte the Soret band at 440 nm is replaced by a band around 460 nm. The magnitude of the Q bands also decreases and a new band appears around 710 nm. After the interaction with an analyte molecule, the energy levels of the conjugated π-electrons in the porphyrin are subsequently shifted and therefore the absorption spectra changes. One of the advantages of using EHO as a sensor is that the spectral change depends upon the number of EHO molecules which have interacted which depends upon the concentration of the analyte. Therefore the level of the EHO response varies with analyte concentration. This spectral characteristic makes the EHO films a useful and selective sensor material.

Fig.2 shows the spectral change of 10 layer EHO LS film after exposure to 855 ppm acetic acid and 900 ppm methylamine vapors. The spectral shift after acetic acid exposure was as expected; similar changes have been recorded before in literature [19]. Exposure to methylamine causes a similar but smaller spectral change and similar results have also been previously recorded against different amines for porphyrin sensor [29-31]. The spectral response observed depends upon the analyte molecule adsorbed and the magnitude of the response depends upon the likelihood of interaction level between the EHO and analyte molecule. The interaction detected is directly related to the physical and chemical properties of the analyte molecule such as its molecular size [19] and active sites present [32]. As seen in

Fig.2 the acetic acid vapor causes a greater response than the methylamine vapor. This could be attributed to a greater binding strength between the porphyrin and the acetic acid vapor in comparison the methylamine vapor. The stronger response of the acetic acid indicates that a greater number of EHO molecules have interacted with the acetic acid molecules than for the methylamine.

Fig.3 shows the kinetic response of LS films with several layers of EHO upon exposure to 855 ppm acetic acid (Fig.3a) and 900 ppm methylamine (Fig.3b). Kinetic measurements were carried out by recording the absorbance change at the constant wavelength of 440 nm (corresponding to the peak of the Soret band) versus time. During the first 10 min period the sensors were exposed to dry nitrogen and at the end of this period vapor molecules were introduced into the exposure chamber. It is clear that the multilayer EHO films have a fast response against to both acetic acid and methylamine vapor. As expected from Fig.2, acetic acid response is larger than methylamine, and it is noted in Fig.3 that it is also faster. During the 20 min exposure cycle EHO films reach the saturation for both vapors. The final magnitude of the response depends on the thickness of the thin film which can be seen to increase with increasing number of layers. The interaction between the vapor and the thin film can be considered in terms of three processes which are surface adsorption, diffusion and desorption process. The surface adsorption causes sharp increase in response immediately after the vapor molecules introduced into the gas cell. Afterwards the vapor molecules start to diffuse into the film structure during which time the sensor response continues to increase but at a slower diffusion limited rate. Gradually during the diffusion limited stage the response starts to settle down until saturation is reached. A dynamic equilibrium and therefore saturation is achieved when the rate of adsorption/desorption and diffusion in/out are in balance. Therefore the magnitude of the initial sharp response and the final saturated response depends on the type of vapor molecules and thin film structure. The final saturation response to methylamine is lower than for acetic acid and the methylamine response takes more time to reach to saturation. This is due to the time taken to reach dynamic equilibrium being longer for the methylamine. In order to obtain quantitative results of the gas sensors, response time (t_{50}) and sensitivity parameters were determined. The t_{50} value gives information about the response time of sensing material and defined as the time taken to get to 50% of the full saturated response. An ideal sensor should be both fast and selective so t_{50} is an important measure of the how fast the sensor material can respond. An alternative measure of response rate is t_{90} which is defined as the time taken for 90% of the total change in absorbance [33]. The magnitude of the maximum saturated absorbance change serves as a measure of the

magnitude of the total sensor response. Table 1 presents the maximum saturated absorbance change and the t_{50}, t_{90} parameters of EHO films. The most remarkable result is that the response time for acetic acid is notably higher than methylamine even though the magnitude of the response is much greater. For instance the 10 layer EHO film upon exposure to acetic acid has a t_{50} value of 49 seconds while methylamine takes 139 seconds. The time difference between two responses is more than twice although the methylamine final response is much lower, approximately half, compared to the acetic acid. When the t_{90} values of 10 layer film are compared, acetic acid response reaches that value in 300 seconds while methylamine takes 499 seconds. The results in Table 1 demonstrate that the EHO sensor has a higher affinity for and therefore sensitivity to acetic acid than methylamine.

In order to provide an explanation of this result based on vapor diffusion and kinetic interactions between thin film and vapor molecules, the Elovichian model was employed [33]. The model states that the vapor adsorption rate or the rate of increase of the surface coverage ($d\Theta/dt$) should decay exponentially as the amount of adsorbed vapor (Θ) increases. The Elovichian equation defined as:

$$d\Theta/_{dt} = A\, exp\{-\beta\Theta\} \tag{3}$$

where A and β are constants. This equation can be integrated in order to express the coverage itself in which:

$$\Theta = \left(1/_{\beta}\right)\ln(t) + K \tag{4}$$

where K is constant. This equation can be interpreted in terms of the probability of adsorption of the vapor molecules decreasing exponentially as a function of the number of the vapor molecules that have already been adsorbed by film surface. Therefore the surface coverage is directly linked to the absorbance change and plots in Fig.4 show the change in the Soret band absorbance versus ln(t). It is clear from the Fig.4 that the relationship is linear until high values of A which corresponds to the surface adsorption. So initially the Elovich model fits the surface adsorption process very well. Then the gradient of the curve is changes indicating that the surface adsorption is completed and a new interaction becomes dominant which is attributed to the diffusion limited response. Therefore the curves in Fig.4 need to be considered in three steps: (1) surface adsorption, (2) diffusion limited and (3) saturation.

Saturation is the flat linear region at the end of interaction which can be clearly seen in all cases. So in order to differentiate between surface and diffusion interactions two gradients have been determined and are given in Table 1. G_1 indicates the first linear part which is dominated by the fast surface interaction and G_2 is the subsequent slower linear region when the diffusion limited response is dominant. The magnitude of the gradient indicates the speed of interaction related to absorbed vapor molecules in time. Table 1 also indicates the duration of each of these stages as t_1 and t_2, surface adsorption and diffusion interactions respectively. It can be clearly seen from the table that the diffusion interactions are considerably slower than the surface adsorption. This is as expected because of the interaction dynamics; as the analyte molecules are required to travel an increasingly tortuous path through the sensor film the diffusion slows the response down, i.e. G2 decreases. Another interesting result is that for the methylamine vapor response it is not as clearly separated in surface and diffusion interactions until the film thickness increases to a 10 layer EHO film. For the lower layer number of EHO films it is difficult to identify two distinct gradients before saturation which is a result of the slower surface interaction and the lower magnitude response between EHO film and methylamine molecules making it more difficult to clearly resolve the two regions of the curves. Thus the surface and diffusion interactions occur simultaneously and it appears in graphs as a curved single step. When surface interaction times (t_1) are compared it can be seen that there is not a big difference between the t_1 times for the different thicknesses of EHO film when considering the acetic acid exposure. This is an expected result because the surface of each film must have similar characteristics and a similar physical structure. As the number of layers and the thickness of the film change the diffusion limited part of the response of vapor molecules is extended, and the total response increased. The t_2 values in Table 1 show the increasing diffusion time with increasing number of EHO layer.

3.2.2 SPR Characterization

Fig.5 shows the shift of the SPR curves for 10 layers of EHO before and after exposure to acetic acid and methylamine vapors. The SPR results correspond with the UV-vis measurements in that the acetic acid interaction causes a bigger change than methylamine vapor. It is clear in Fig.5 that acetic acid causes an SPR minima shift of about 1.9^o and the methylamine shift is only about 0.7^o when a 10 layer EHO film is exposed. Table 2 presents the angular shift of the SPR minima for each EHO film after exposure to acetic acid and methylamine. The shift of the SPR curve minima is a result of the level of interaction between

organic film and vapor molecule. So the SPR sensing experiments are in strong agreement with the results observed in the UV-Vis experiments. Both experiments suggest that acetic acid and methylamine vapor molecules interact with EHO film, and the acetic acid interaction is greater in magnitude.

Fig.6 presents the kinetic SPR results of EHO films exposed to 855 ppm of acetic acid (Fig.6a) and 900 ppm of methylamine vapor (Fig.6b), where the normalized reflected light intensity is plotted as a function of time at the SPR angle of 49^{o}. During the dynamic experiments the EHO LS films were exposed to organic vapors in the gas cell for 20 min followed by clean dry air for a further 10 min. Injection of the vapors causes a sharp increase for a few seconds and then the responses decrease exponentially until a saturation point is reached. This has been observed previously and has been attributed to initial vapor condensation on the film surface as a result of the injection process used [34]. When dry air is subsequently injected into gas cell, the reflected light intensity returns back to its initial value. The responses of the EHO films are both fast and reversible upon exposure to both vapors. Again it is noted that the response rate for the exposure to acetic acid is faster than when exposed to methylamine. The response time is approximately 1 second which is a sufficiently fast for a good sensor device. The recovery time is about 3 seconds and fully recovery can be achieved by simply injecting clean dry air.

It is clear from the kinetic measurements that the sensing response increases with increasing number of EHO layer which indicates that the vapor diffuses into the bulk film structure. This dependence between thickness and the magnitude of response is beneficial as it provides a simple mechanism to increase the strength of the sensor signal. As with the UV-vis data, the SPR data can be better understood by considering the interaction between the vapor and the organic film. It starts with the surface adsorption of the analyte which causes a sudden response increase within a fraction of a second. The surface interaction is a fast response because there are no obstacles in the way and therefore is a good indicator of the presence of the vapor molecules. When we consider the sharp increase of SPR curve after injection of vapors, it can be seen that the acetic acid interaction with the film surface is stronger and faster than for methylamine. The faster initial response reported for the SPR data is thought to be related to the fast injection process used to deliver the analyte which may result in a thin film of analyte momentarily condensing onto the sensor film surface [34]. In the case of the UV-vis experiments the flow is switched from clean N_2 to N_2 with analyte so the initial response rate is influenced by the time taken to fill the exposure chamber. After the easily accessible EHO molecules on film surface are have all been exposed to the analyte the rapid

surface adsorption process reaches completion and then the slower diffusion limited interaction mechanism becomes dominant. Vapor molecules which are diffusing into the film structure can access the lower layers of EHO within the film. Eventually the response of the thin film starts to settle down to a dynamic equilibrium. During the diffusion limited stage, adsorption and desorption of vapor molecules and diffusion in and out of the sample occur simultaneously. Diffusion of the vapor molecules depends on several parameters because there is a partially obstructed path for the vapor molecules which slows down the sensor response. This change of the sensor response speed is a distinctive and useful characteristic for the interaction mechanism. Vapor molecules which have diffused into the film are adsorb onto the thin film molecules inside the structure thus the swelling of thin film occurs. SPR is a perfect system to monitor the swelling as a function of time. Therefore swelling behavior has been investigated in order to clarify the diffusion effect.

Fig.7 shows the normalized photo detector response (I_{rf}/I_o) against swelling time (t_s) where the t=0 represents the start of vapor exposure. It is clear from the Fig.7 that the I_{rf} decreases while the vapor exposure time increases. The rate of the decrease of I_{rf} varies depending on the introduced vapor into gas cell. This can be explained by the penetrating vapor molecules moving into thin film structure and increasing the film transparency. The decrease of the I_{rf} continues until the saturation point where the diffusion of vapor molecules eventually reaches dynamic equilibrium when adsorption is matched by desorption and diffusion in by diffusion out. So the time until saturation defines the swelling time that is the time taken for the vapor molecules to diffuse into the film. Table 2 gives the swelling times for each of the samples for each analyte vapor.

As seen in Fig.7a, the swelling time increases with increasing number of layers. Similar behavior is observed in the case of methylamine in Fig.7b. The swelling time can be correlated with the interaction time which starts with exposure and continues until saturation. The thicker films have a larger volume of structure for the vapor molecules to diffuse through resulting in larger swelling times for thicker films. The specific analyte vapor molecule also influences the swelling characteristics. When Fig.7a and Fig.7b are compared, methylamine swelling time is notably longer than acetic acid when considering films with equal number of layers. Although the final saturated response magnitude is lower, methylamine diffusion takes a longer time and increases the swelling time. This is a result of the different interaction mechanisms of the two analyte molecules. Considering these results, methylamine EHO film interaction is weaker and diffusion of vapor is slower than acetic acid. This is somewhat surprising given that the concentrations used were similar and acid and the amine molecules

are similar in size. One possible explanation is that the acidic nature of the acid helps it to penetrate between aggregated porphyin molecules resulting in a faster and stronger response. Adsorption of the vapor molecules by the thin film matrix causes the swelling and thus the thickness of the film to increases during the swelling process. Table 2 presents the thickness changes of the samples after exposure to the analyte vapors.

The change of the I_{rf} can be related to the quantity of the analyte molecules (M_t) which have penetrated into thin film matrix. Fick's second law of diffusion describes this relation and means that the rate of change in concentration with time is proportional to the rate at which the concentration gradient changes with the distance in a given direction [35]. The simplified form of the diffusion equation can be defined by the following equation [18]:

$$\frac{M_t}{M_\infty} = 4\sqrt{\frac{D}{\pi a_0^2}}\, t_s^{1/2} \tag{5}$$

where a_0 is the thickness, D is the diffusion coefficient, M_t and M_∞ represent the amount of diffusant entering the plane sheet at time t and infinity, respectively and t_s represents the swelling time.

The amount of the vapor penetrating into film M_t is inversely proportional to the reflected light intensity I_{rf}. So the Eq. (5) can be written as:

$$\left(\frac{M_t}{M_\infty}\right) \sim \left(\frac{I_{rf(t)}}{I_{rf(\infty)}}\right)^{-1} = 4\sqrt{\frac{D}{\pi a_0^2}}\, t_s^{1/2} \tag{6}$$

where $I_{rf(t)}$ is the reflected light intensity at any time and $I_{rf(\infty)}$ is the reflected light intensity of the saturation point.

Fig.8 depicts the normalized intensity of reflected light versus the square root of the swelling time. Diffusion coefficients (D_s) for every step can be determined from the gradients of the linear sections in relation with Eq. (4) and these are plotted in the insets in Fig.8. The correlation between the number of layer in each film and D_s of acetic acid is shown in inset of Fig.8a. Since the gradients in figures 8a and 8b are all quite similar it appears that the changes in the film thickness squared (a_0^2) are largely matched by changes in the diffusion coefficient D. This can be understood in that as the film swells it will create more available free space and become more open and therefore diffusion occurs more rapidly. It is clear that the

diffusion coefficient of acetic acid increases with increasing number of layer. The bigger value of diffusion coefficient corresponds to the fast diffusion. Similar behavior is recorded in the case of methylamine. Although the correlation between thickness and D_s is almost linear for methylamine vapor, whereas this exhibits an exponential increase in the case of acetic acid. This supports the argument that the diffusion coefficient is directly dependent on the analyte vapor.

In order to obtain quantitative results about sensor performance, the sensitivity (S) and the limit of detection (LOD) parameters were calculated and summarized in Table 3. The change of response per exposed vapor ppm gives the sensitivity value. It was estimated from the change of Absorbance at 440 nm per ppm (A/ppm) for UV-vis results. The sensitivity of the SPR results was estimated from the reflected light intensity change per ppm (I_{rf}/ppm) at the SPR angle of 49°. The limit of detection implies the lowest quantity (ppm) of the analyte that can be detected by the sensor and described by the following equation [22]:

$$\mathrm{LOD} = \frac{3\sigma}{\mathrm{S}} \tag{7}$$

where σ is the standard deviation of the signal.

As seen on Table 3, EHO sensor system is more sensitive to acetic acid then methylamine. Furthermore the sensitivity of the sensor system increases with increasing number of layers against both analyte. This is a predictable result because of the increasing magnitude of response of multilayer EHO films results in a better signal to noise ratio for thicker films. Another interesting result in Table 3 is the dependence of sensitivity to the measurement technique. In UV-vis measurements, the sensitivities of the EHO are in the range of 10^{-4} ppm^{-1} which is much lower in SPR results around 10^{-7} ppm^{-1}. So the experimental setup and measured physical property resulting from the vapor interaction has a significant effect on the sensitivity. But if we consider the LOD values; there are no significant differences between UV-vis and SPR measurements. LOD values of acetic acid estimated from UV-vis setup are in the range of ~12-25 ppm which are ~6-40 ppm for SPR measurements. In the case of methylamine sensing, UV-vis results give LOD values in the range between ~24-135 ppm, SPR data give ~13-108 ppm. There is an inverse proportionality between film thickness and LOD values as seen in Table 3. The decrease in LOD with increasing number of layers is observed for both systems. This indicates that it is possible to detect a lower ppm of analyte

vapor by increasing number of EHO layers. This is a very important consideration when seeking to design highly sensitive gas sensors.

4. Conclusion

The aim of this study was to investigate the sensor response of multilayer porphyrin LS films upon exposure to both acidic and basic organic vapors in order to compare the performance of the sensing films when measured by either UV-vis or SPR. EHO was chosen for the active layer of the vapor sensor and multilayer films were produced via Langmuir-Schaefer technique. Films of 4, 6, 8 and 10 layers of LS films were successfully produced and the thickness was determined to be between 66-314 Å depending on the number of layers. The films were exposed to acetic acid and methylamine until the sensor response reached saturation point. In order to perform a comparative study, kinetic measurements were carried out using both UV-vis and SPR measurements systems. Both of the techniques are based on optical measurements however UV-vis measures the spectral changes while SPR evaluates the thickness change and swelling of the thin film. Using two different sensing techniques gives an opportunity to check the relative sensitivity of each sensor system and to make comparisons in order to further understanding of the adsorption kinetics. The results obtained show that EHO sensors demonstrate significant responses to both acetic acid and methylamine. In the UV-vis experiments the spectral response to the acid was very similar to the response to the base, and for the SPR the swelling responses were also similar. For both the UV-vis and the SPR the acetic acid caused a larger response and therefore it can be said EHO as a sensor is more sensitive to acetic acid than methylamine. In addition, as was expected the sensor response increases with increasing film thickness because an increasing number of EHO molecules are available for interaction. It is shown that the results obtained from UV-vis and SPR are consistent with the theory that the sensor response consists of two main interactions which are a fast surface interaction followed by a slower diffusion limited response as the vapors penetrate deeper into the films. The response speed depends on the specific interaction occurring on the films and the diffusion rate of the analyte vapor through the films. SPR results show that adsorption of vapor molecules by the film matrix causes swelling of the film so the thickness of film increases. The rate of swelling is directly related with the analyte vapor and initial thickness of the film. Our results showed that the sensitivity of the sensor is largely independent from the measurement system provided it is sufficiently

sensitive to measure the physical parameters which are changing and the interaction process consists of two different stages.

Acknowledgments

The authors would like to thank Professor Chris Hunter & Jordan Hutchinson from the Chemistry Department at the University of Sheffield, for synthesizing the porphyrin used in this work. M. Evyapan also thanks Turkish High Education Council (YOK) for the Post. Doc. scholarship. A. Dunbar would like to acknowledge support from a Royal Society: Ultrathin Polymer Membranes research grant.

References

[1] D. Xu, M. Guan, Q. Xu, Y. Guo, Multilayer films of layered double hydroxide/polyaniline and their ammonia sensing behavior, J. Hazard.Mater. 262 (2013) 64-70.

[2] L.F. da Silva, V.R. Mastelaro, A.C. Catto, C.A. Escanhoela, S. Bernardini, S.C. Zilio, E. Longo, K. Aguir, Ozone and nitrogen dioxide gas sensor based on a nanostructured SrTi0.85Fe0.15O3 thin film, J. Alloys and Compounds 638 (2015) 374-379.

[3] T. Hyodo, C. Ishibashi, K. Matsuo, K. Kaneyasu, H. Yanagi, Y. Shimizu, CO and CO_2 sensing properties of electrochemical gas sensors using an anion-conducting polymer as an electrolyte, Electrochimica Acta 82 (2012) 19-25.

[4] I.A. Koshets, Z.I. Kazantseva, Yu.M. Shirshov, S.A. Cherenok, V.I. Kalchenko, Calixarene films as sensitive coatings for QCM-based gas sensors, Sens. Actuators B 106 (2005) 177-181.

[5] B. Wang, L. Zhang, B. Li, Y. Li, Y. Shi, T. Shi, Synthesis, characterization, and oxygen sensing properties of functionalized mesoporous silica SBA-15 and MCM-41 with a Pt(II)–porphyrin complex, Sens. Actuators B: Chem. 190 (2014) 93-100.

[6] B. Wang, X. Zuo, Y. Wu, Z. Chen, C. He, W. Duan, Comparative gas sensing in copper porphyrin and copper phthalocyanine spin-coating films, Sens. Actuators B: Chem. 152 (2011) 191-195.

[7] A.J. McNaughton, A. Dunbar, W. Barford, T.H. Richardson, Modeling the Kinetics of Gas Adsorption in Multilayer Porphyrin Films, Langmuir 2007, 23, 1759-1767.

[8] A.F. Gutiérrez, S. Brittle, T.H. Richardson, A. Dunbar, A proto-type sensor for volatile organic compounds based on magnesium porphyrin molecular films, Sens. Actuators B:Chem 202 (2014) 854-860.

[9] B. Wang, X. Zuo, Y.Q. Wu, Z.M. Chen, Preparation, characterization and gas sensing properties of lead tetra-(tert-butyl)-5,10,15,20-tetraazaporphyrin spin-coating films, Sens. Actuators B: Chem. 125 (2007) 268-273.

[10] S.T. Kang, H. Ahn, Dicyanopyrazine-linked porphyrin Langmuir–Blodgett films, J. Colloid and Interface Sci. 320 (2008) 548-554.

[11] S.A. Brittle, T.H. Richardson, A.D.F. Dunbar, S. M.Turega, C.A. Hunter, Tuning free base tetraphenylporphyrins as optical sensing elements for volatile organic analytes, J. Mater. Chem.21 (2011) 4882-4887.

[12] M.G. Manera, E.F. Vila, A. Cebollada, J.M.G. Martín, A.G. Martín, G. Giancane, L. Valli, R. Rella, Ethane-Bridged Zn Porphyrins Dimers in Langmuir−Schäfer Thin Films:

Spectroscopic, Morphologic, and Magneto-Optical Surface Plasmon Resonance Characterization, J. Phys. Chem. C 2012, 116, 10734-10742.

[13] J. Roales, J.M. Pedrosa, M.G. Guillén, T.L. Costa, S.M.A. Pinto, M.J.F. Calvete, M.M. Pereira, Optical detection of amine vapors using ZnTriad porphyrin thin films, Sens. Actuators B 210 2015, 28-35.

[14] A.A Alwahib, A.R. Sadrolhosseini, M.N. An'amt, H.N. Lim, M.H. Yaacob, M.H. Abu Bakar, H.N. Ming, M.A. Mahdi, Reduced Graphene Oxide/Maghemite Nanocomposite for Detection of Hydrocarbon Vapor Using Surface Plasmon Resonance, IEEE Photonics Journal 8 2016, 4802009.

[15] A.D.F. Dunbar, T.H. Richardson, J. Hutchinson, C.A. Hunter, Langmuir–Schaefer films of five different free base tetraphenylporphyrins for optical-based gas sensing of NO2, Sens. Actuators B: Chem. 128 (2008) 468-481.

[16] E. Kretschmann, H. Raether, Z. Naturforsch. 23a (1968) 2135-2136.

[17] A.V. Nabok, A.K. Hassan, A.K. Ray, O. Omar, V.I. Kalchenko, Study of adsorption of some organic molecules in calix[4]resorcinolarene LB films by surface plasmon resonance, Sens. Actuators B 45 (1997) 115–121.

[18] M. Evyapan, B. Kadem, T.V. Basova, I.V. Yushina, A.K. Hassan, Study of the sensor response of spun metal phthalocyanine films to volatile organic vapors using surface plasmon resonance, Sens. Actuators B 236 (2016) 605–613.

[19] M. Evyapan, A.D.F. Dunbar, Controlling surface adsorption to enhance the selectivity of porphyrin based gas sensors, Applied Surface Science 362 (2016) 191–201.

[20] D. Mackay, W.Y. Shiu, K.C. Ma, S.C. Lee, Physical-Chemical Properties and Environmental Fate for Organic Chemicals, CRC Press Taylor & Francis Group, Boca Raton FL, 2006, pp 2687-2778.

[21] H. Banimuslem, A. Hassan, T. Basova, A.A. Esenpınar, S. Tuncel, M. Durmus, A.G. Gürek, V. Ahsen, Dye-modified carbon nanotubes for the optical detection of amines vapors, Sens. Actuators B 207 (2015) 224-234.

[22] M. Evyapan, A.D.F. Dunbar, Improving the selectivity of a free base tetraphenylporphyrin based gas sensor for NO_2 and carboxylic acid vapors, Sens. Actuators B: Chem. 206 (2015) 74-83.

[23] S.A. Brittle, A. Flores, A. Hobson, A.J. Parnell, A.D.F. Dunbar, C.A. Hunter, T.H. Richardson, Macroscopic expansion of tetraphenylporphyrin Langmuir layers stimulated by protonation, Soft Matter8 (2012) 2807-2811.

[24] A.D.F. Dunbar, T.H. Richardson, J. Hutchinson, C.A. Hunter, Langmuir–Schaefer films of five different free base tetraphenylporphyrins for optical-based gas sensing of NO_2, Sens. Actuators B: Chem. 128 (2008) 468-481.

[25] A.V. Nabok, A.K. Hassan, A.K. Ray, O. Omar, V.I. Kalchenko, Study of adsorption of some organic molecules in calix[4]resorcinolarene LB films by surface plasmon resonance, Sens. Actuators B 45 (1997) 115–121.

[26] A.K. Ray, O. Omar, C.S. Bradley, N.A. Bell, D.J. Simmonds, C.S. Thorpe, R.A. Broughton, Vacuum 57 (2000) 253-258.

[27] A.V. Nabok, A.K. Hassan, A.K. Ray, O. Omar, V.I. Kalchenko, Sens. Actuators B 45 (1997) 115-121.

[28] A. Dunbar, T.H. Richardson, A.J. McNaughton, W. Barford, J. Hutchinson, C.A. Hunter, Understanding the interactions of porphryin LB films with NO2, Colloids Surf. A: Physicochem. Eng. Asp. 284-285 (2006) 339-344.

[29] S.A. Brittle, T.H. Richardson, J. Hutchinson, C.A. Hunter, Comparing zinc and manganese porphyrin LB films as amine vapour sensing materials, Colloids Surf. A: Physicochem. Eng. Asp. 321 (2008) 29-33.

[30] S.A. Brittle, T.H. Richardson, A.D.F. Dunbar, S.M. Turega, C.A. Hunter, Tuning free base tetraphenylporphyrins as optical sensing elements for volatile organic analytes, J. Material. Chem. 21 (2011) 4882-4887.

[31] A.D.F. Dunbar, S. Brittle, T.H. Richardson, J. Hutchinson, C.A. Hunter, Detection of Volatile Organic Compounds Using Porphyrin Derivatives, J. Phys. Chem. B 114 (2010) 11697-11702.

[32] C.M. Dooling, T.H. Richardson, Thickness dependence of the toxic gas response in EHO Langmuir–Blodgett films prepared by ultra-fast deposition, Mater. Sci. Eng. C 22 (2002) 269-274.

[33] T.H. Richardson, C.M. Dooling, L.T. Jones, R.A. Brook, Development and optimization of porphyrin gas sensing LB films, Adv. Colloid Interface 116 (2005) 81-96.

[34] A.V. Nabok, A.K. Hassan, A.K. Ray, Condensation of organic vapours within nanoporous calixarene thin films, J.Mater.Chem.10 (2000) 189-194.

[35] J. Crank, The Mathematics of Diffusion, Oxford University Press, London, 1975.

Biographies

Murat Evyapan, BSc, MSc, PhD in Physics, is a research assistant at the Department of Physics at University of Balikesir. He received his MSc and PhD in physics from Balikesir University, Turkey in 2006 and 2012. He had a Post. Doc. scholarship from Turkish High Education Council in 2013 for Abroad Research in UK. He worked as a Post. Doc. Researcher in University of Sheffield, UK for one year. His main interests are organic thin films and gas sensor for environment applications.

Aseel Hassan, BSc, MSc, PhD in Physics, is a Reader at the Materials and Engineering Research Institute of Sheffield Hallam University, UK. He carries out his research with main interest lies in thin film technology mainly for application in chemical and biosensing. He uses optical techniques such as surface plasmon resonance and spectroscopic ellipsometry, as well as quartz crystal microbalance detection techniques, employing organic films such as metallophthalocyanines and calix-resorcinarenes as the sensing layers. Dr Hassan also specialises in physical electronics and focuses mainly on solar cells research and development.

Alan Dunbar attained an MPhys in Physics with Electronics in 1997, and his PhD in 2001 from UMIST (Manchester). After his PhD, he moved to the University of Canterbury, Christchurch NZ where he worked as a research fellow for two years. He then returned to the UK and began working at the University of Sheffield (Department of Physics and Astronomy). In 2009 he was appointed as Lecturer in Energy, in the Department of Chemical and Biological Engineering at the University of Sheffield, and became a Senior Lecturer in Energy in 2014. His research interests include organic gas sensors, organic photovoltaics and nanostructured materials.

Figure Caption

Fig. 1. SPR curves of different number of layer EHO LS films as a function of internal angle.

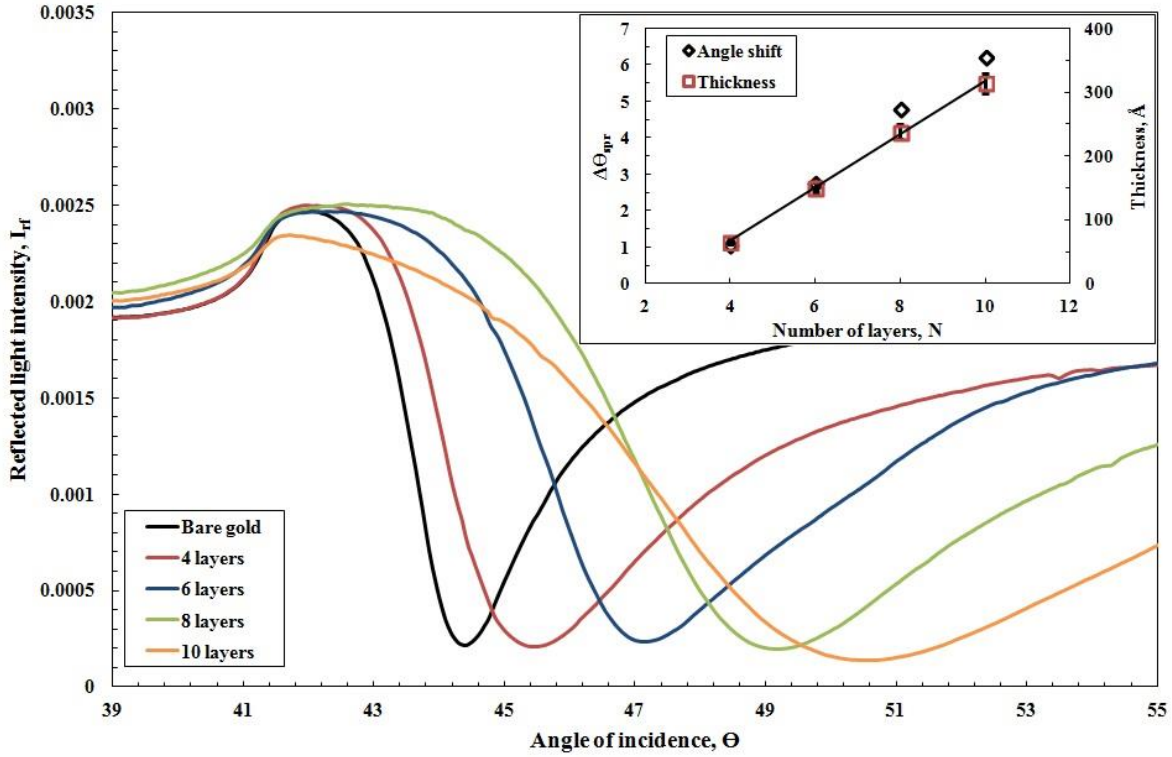

Fig. 2. The UV absorption spectra of 10 layer EHO LS film upon exposure to 855 ppm acetic acid and 900 ppm methylamine vapors.

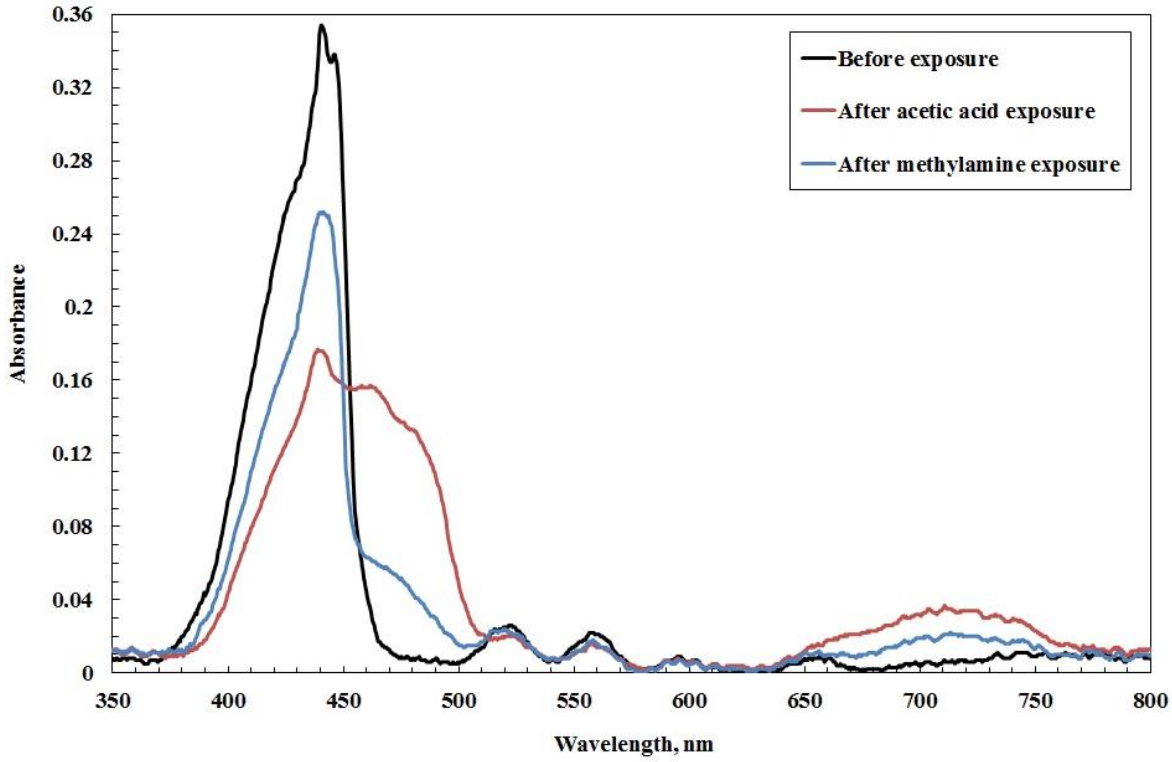

Fig. 3. The kinetic UV absorbance change of several layers EHO LS films upon exposure to (a) 855 ppm acetic acid vapor, (b) 900 ppm methylamine vapor.

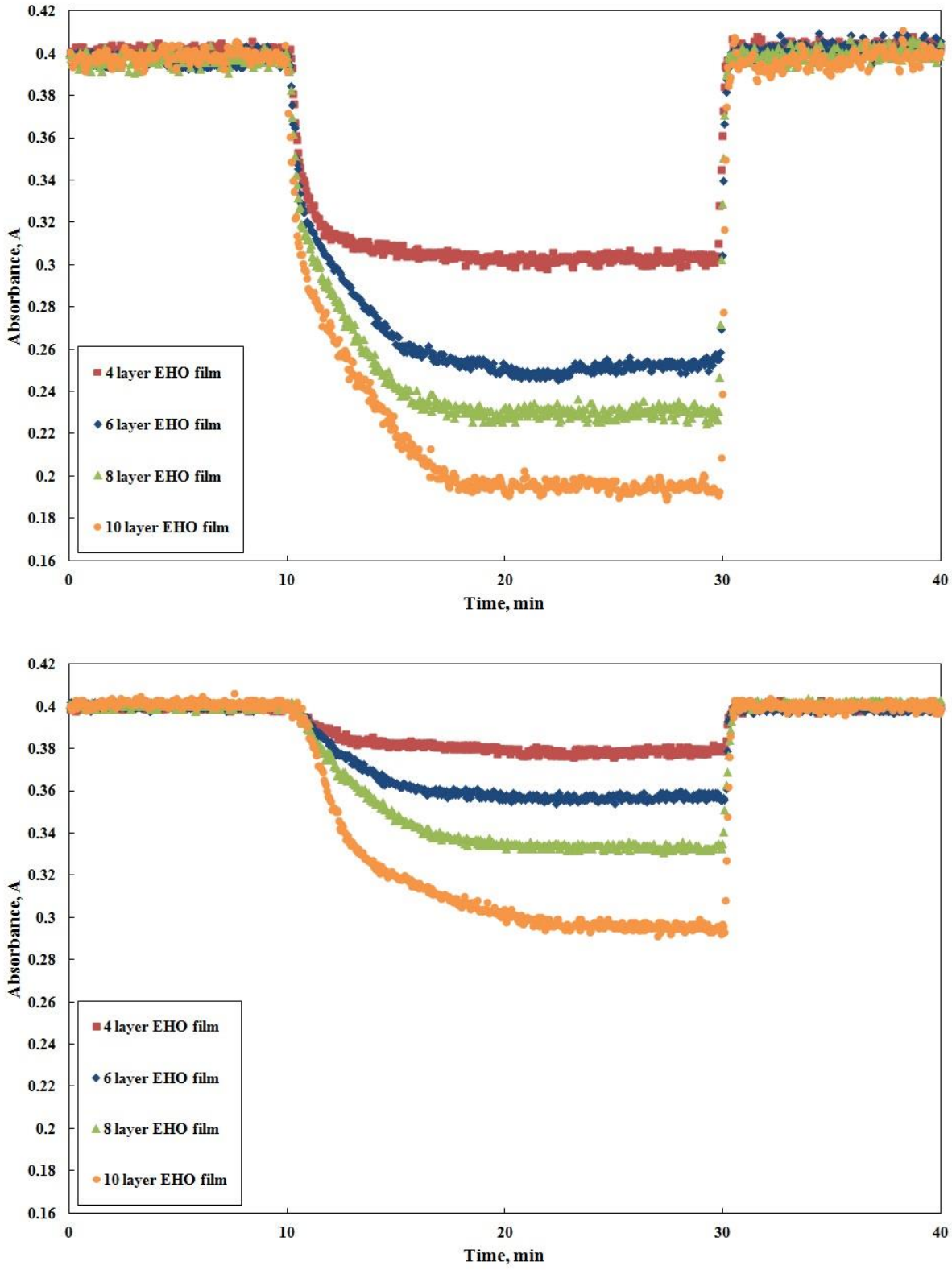

Fig. 4. Elovich response kinetics for the several layers EHO LS films upon exposure to (a) 855 ppm acetic acid vapor, (b) 900 ppm methylamine vapor.

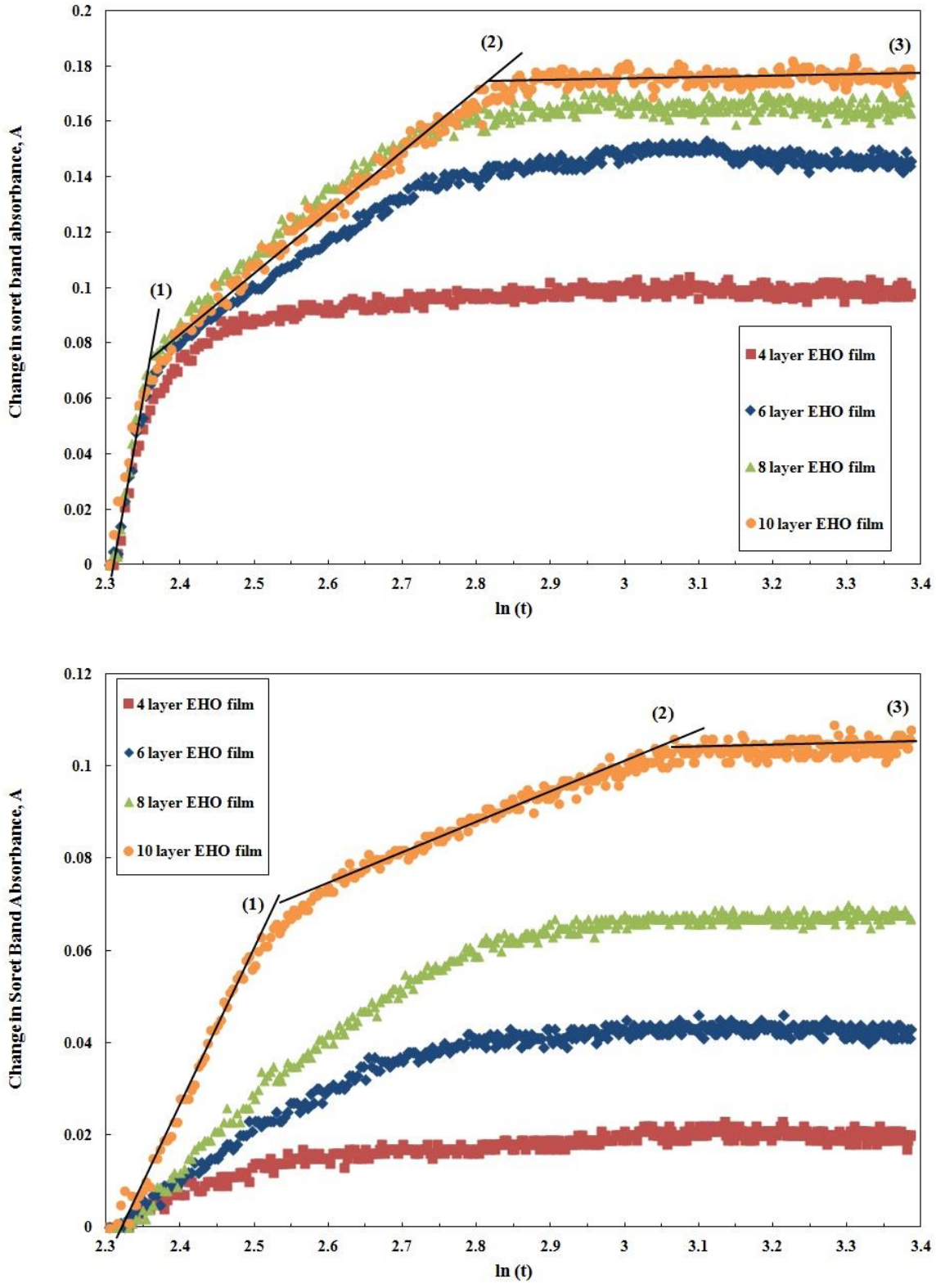

Fig. 5. SPR curves of 10 layer EHO LS film before and after exposure to acetic acid (855 ppm) and methylamine (900 ppm) vapors.

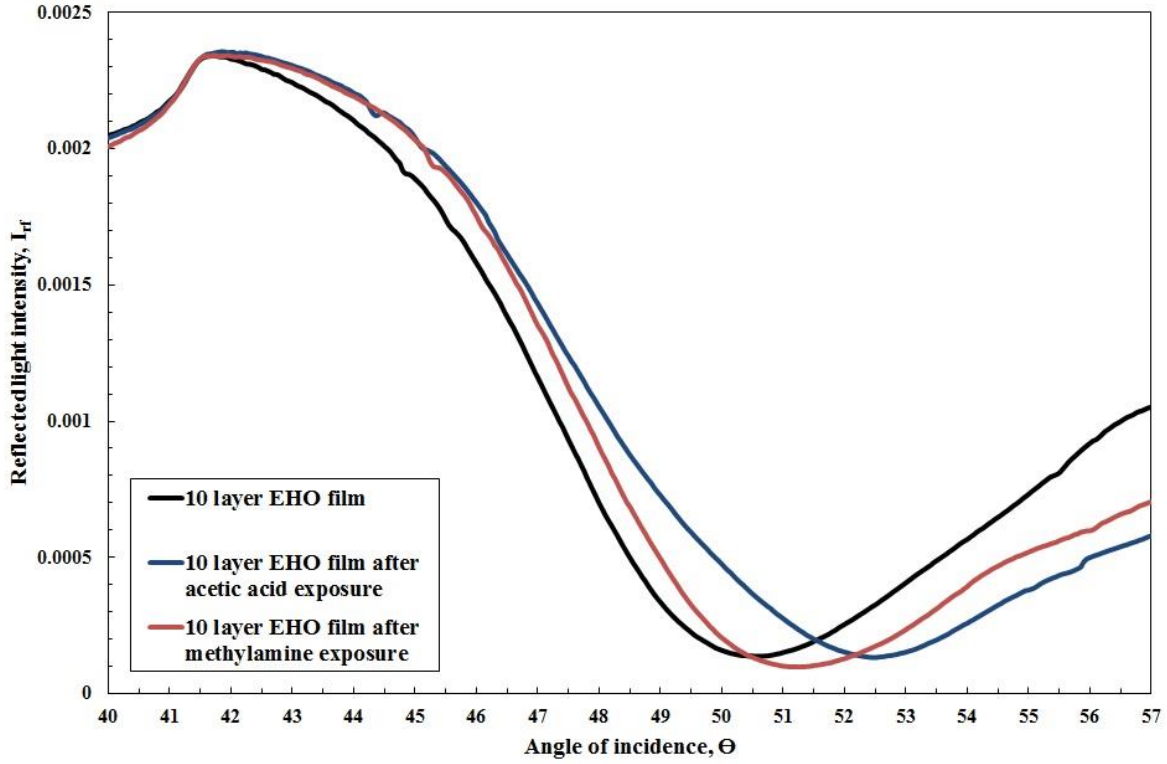

Fig. 6. The kinetic SPR measurements of several layers EHO LS films upon exposure to (a) 855 ppm acetic acid vapor, (b) 900 ppm methylamine vapor.

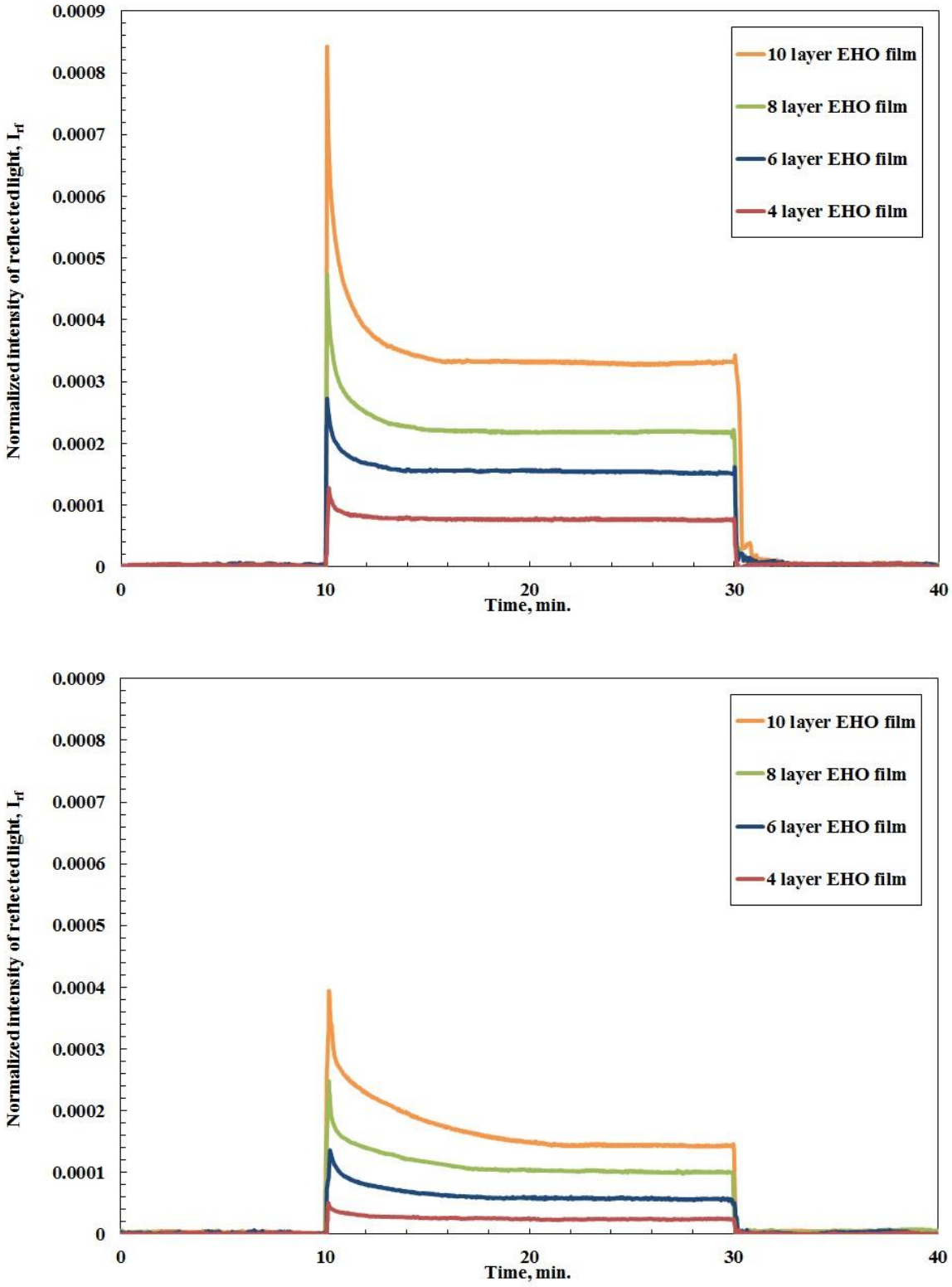

Fig. 7. Normalized photo detector response, (I_{rf}/I_0) against swelling time, (t_s) for the several layers EHO LS films upon exposure to (a) 855 ppm acetic acid vapor, (b) 900 ppm methylamine vapor.

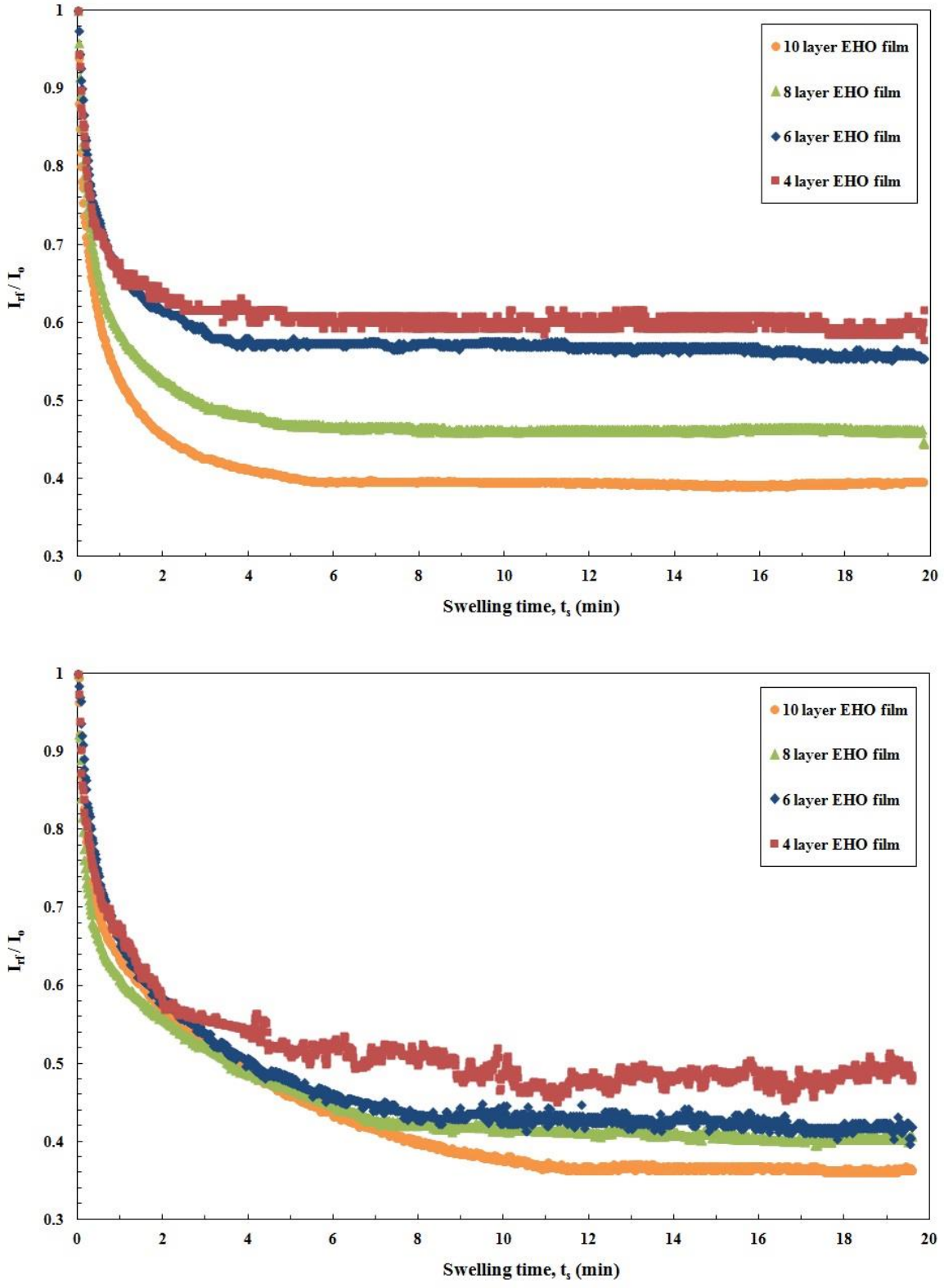

Fig. 8. Plot of reflected light intensity against square root of swelling time for the several layers EHO LS films upon exposure to (a) 855 ppm acetic acid vapor, (b) 900 ppm methylamine vapor.

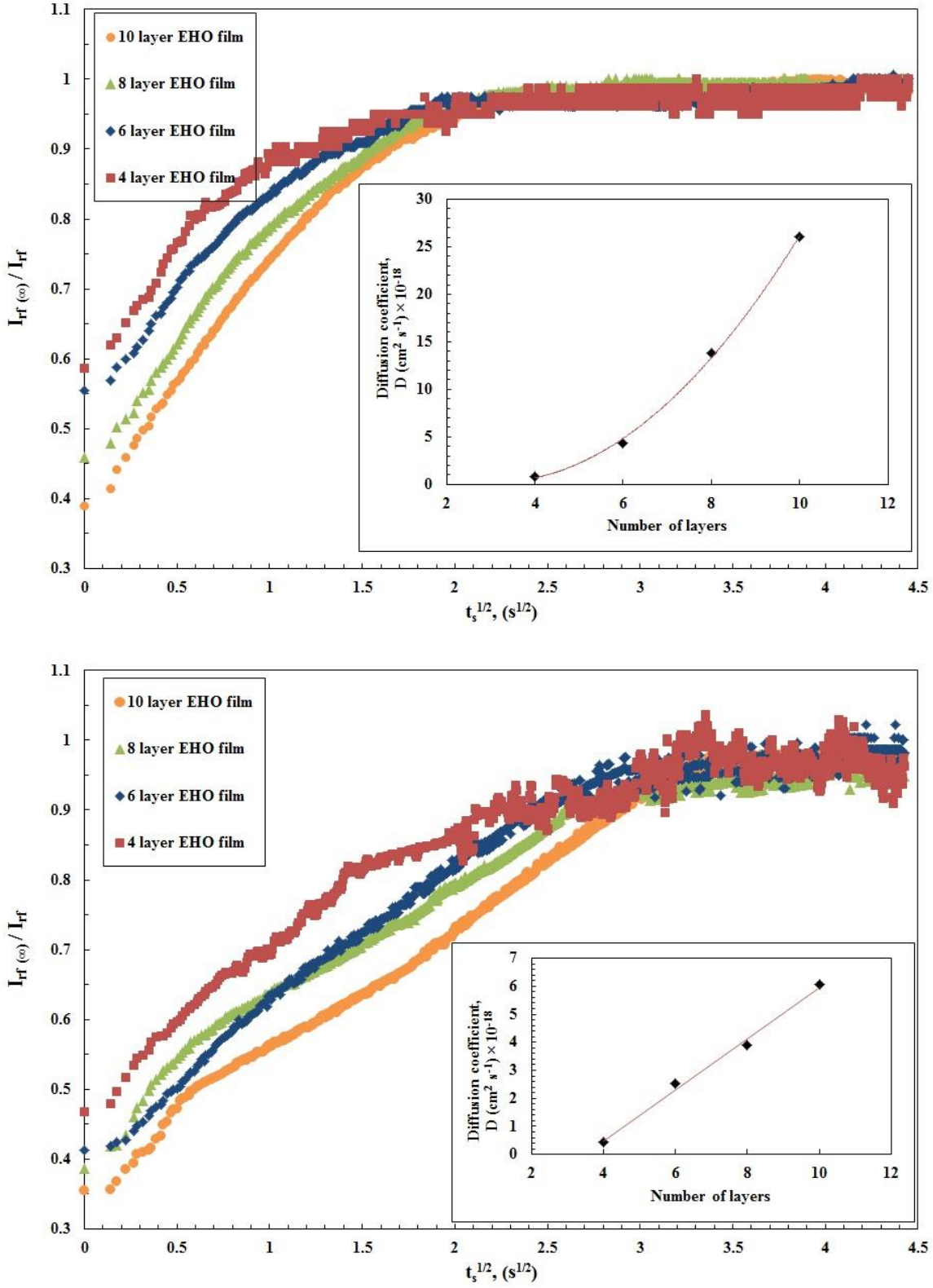

Table 1: Sensing analysis of UV-vis results

	4 layers		6 layers		8 layers		10 layers	
	Acetic acid	**Methylamine**	**Acetic acid**	**Methylamine**	**Acetic acid**	**Methylamine**	**Acetic acid**	**Methylamine**
Max Abs. change	0.100	0.021	0.147	0.044	0.170	0.068	0.206	0.106
t_{50} (s)	30	76	42	133	45	137	49	139
t_{90} (s)	156	276	270	352	284	397	300	499
G_1 (gradient)	1.09	0.06	1.23	0.10	1.25	0.12	1.25	0.33
t_1 (s)	~39	~154	~40	~243	~43	~376	~43	~123
G_2 (gradient)	0.17	-	0.17	-	0.20	-	0.21	0.06
t_2 (s)	~57	-	~243	-	~316	-	~327	~495

Table 2: SPR analysis of thin films

	4 layers		6 layers		8 layers		10 layers	
Thickness of LS films (Å)	66		151		238		314	
Analyte vapors	**Acetic acid**	**Methylamine**	**Acetic acid**	**Methylamine**	**Acetic acid**	**Methylamine**	**Acetic acid**	**Methylamine**
Swelling time (s)	147	388	214	480	285	483	334	654
SPR shift after exposure ($\Delta\Theta^o$)	0.35	0.15	0.95	0.30	1.00	0.55	1.95	0.70
Thickness change after exposure (Å)	~15	~7	~39	~12	~41	~18	~81	~24

Table 3: Sensitivity and LOD parameters of multilayer sensor systems

		4 layers		6 layers		8 layers		10 layers	
Analyte vapors		**Acetic acid**	**Methylamine**	**Acetic acid**	**Methylamine**	**Acetic acid**	**Methylamine**	**Acetic acid**	**Methylamine**
UV-Vis	**S (ppm^{-1}) $\times 10^{-4}$**	1.17	0.22	1.75	0.44	1.99	0.77	2.46	1.22
	LOD (ppm)	25.65	135.00	17.10	67.50	15.09	38.57	12.21	24.55
SPR	**S (ppm^{-1}) $\times 10^{-7}$**	1.50	0.55	3.18	1.50	5.52	2.76	9.82	4.38
	LOD (ppm)	40.08	108.00	18.86	40.00	10.87	21.77	6.11	13.71